SCIENCE CHINA
Physics, Mechanics & Astronomy

• Article •

doi: 10.1007/s11433-014-5460-y

Plasmonic-enhanced two-photon fluorescence with single gold nanoshell†

ZHANG TianYue[1], LU GuoWei[1*], SHEN HongMing[1], Perriat P[2], Martini M[3], Tillement O[3] & GONG QiHuang[1,4]

[1] *State Key Laboratory for Mesoscopic Physics, Department of Physics, Peking University, Beijing 100871, China;*
[2] *Matériaux, Ingénierie et Sciences (MATEIS), UMR 5510 CNRS, INSA-Lyon, Université de Lyon, Villeurbanne Cedex 6962, France;*
[3] *CNRS Laboratory of Physio-Chemistry of Luminescent Materials, Université de Lyon, Université Claude Bernard, Villeurbanne Cedex 69622, France;*
[4] *Collaborative Innovation Center of Quantum Matter, Beijing 100871, China*

Received February 25, 2014; accepted March 13, 2014

Single gold nanoshell with mutilpolar plasmon resonances is proposed to enhance two-photon fluorescence efficiently. The single emitter single nanoshell configuration is studied systematically by employing the finite-difference time-domain method. The emitter located inside or outside the nanoshell at various positions leads to a significantly different enhancement effect. The fluorescent emitter placed outside the nanoshell can achieve large fluorescence intensity given that both the position and orientation of the emission dipole are optimally controlled. In contrast, for the case of the emitter placed inside the nanoshell, it can experience substantial two-photon fluorescence enhancement without strict requirements upon the position and dipole orientations. Metallic nanoshell encapsulating many fluorescent emitters should be a promising nanocomposite configuration for bright two-photon fluorescence label. The results provide a comprehensive understanding about the plasmonic-enhanced two-photon fluorescence behaviors, and the nanocomposite configuration has great potential for optical detecting, imaging and sensing in biological applications.

surface plasmon resonances, two-photon fluorescence, finite-difference time-domain

PACS number(s): 73.22.-f, 33.50.-j, 02.70.Bf

Citation: Zhang T Y, Lu G W, Shen H M, et al. Plasmonic-enhanced two-photon fluorescence with single gold nanoshell. Sci China-Phys Mech Astron, doi: 10.1007/s11433-014-5460-y

1 Introduction

Two-photon excitation fluorescence is growing in popularity in the bioimaging field because of its high confinement excitation, intrinsic three dimensionality of images, and reduced photodamage to living organisms when compared to one-photon processes [1,2]. However, one of the disadvantages of using two-photon excitation is fluorophores' extremely low two-photon absorption cross-section. The demand for developing efficient fluorescent probes with improved two-photon fluorescence (TPF) properties has triggered extensive studies in recent years. Many of the efforts are in the synthesis of fluorescent probes with large two-photon absorption cross-section [3]. Meanwhile, the nanocomposite type of fluorescent nanoparticles have received increasing attention because of their attractive optical properties. Dye-loaded fluorescent nanoparticles are widely used. They are designed such that the dye molecules are encapsulated into the polymeric matrices, such as silica, dextran, polystyrene, etc. [4]. Fluorescent quantum dots and

*Corresponding author (email: guowei.lu@pku.edu.cn)
†Contributed by GONG QiHuang (Executive Associate Editor-in-Chief)

quantum rods are also reported to have the sufficient two-photon excitation efficiency used for two-photon bioimaging [4–6]. The strategy of using metallic nanoparticles to achieve the TPF enhancement is another appealing scheme, which is based on the interactions between the fluorophores and the plasmonic nanoparticles. Compared to the metallic nanostructures fabricated on the substrate [7,8], metallic nanoparticles have more flexibility and much smaller dimensions, which are desirable as free diffusion labels in biological imaging and sensing. Also, various types of surface fictionalization of the metal surface enable metallic nanoparticles to be more versatile two-photon probes for specific applications. The effective coupling between fluorophores and the localized surface plasmon resonances (LSPRs) of metallic nanoparticles results in enhanced fluorescence intensity, shortened fluorescence lifetime and extended photoresistance of the fluorescence behaviors [9–18]. In comparison with the traditional organic-based fluorescent dyes, proteins, and fluorescent quantum dots, fluorescent metallic nanoparticles offer much improved sensitivity and photostability.

Among various types of metal nanoparticles, metallic nanoshells are especially suitable as the carriers of fluorescent emitters to construct composited TPF probes, because their plasmon resonance bands easily span the near-infrared region where biological tissues display minimal autofluorescence and absorption. The nanoshells act as optical antenna enabling the local field enhancement, the increase in radiative decay rate of the fluorophore that alters the quantum efficiency, and modulation of the far-field radiative coupling of fluorescence emission through nanoparticle scattering. Also, the core shell structure offers a platform for designing and fabricating multifunctional nanoparticles. A metallic nanoshell (NS) comprising a dielectric core (silica) surrounded by a thin metallic shell (gold or silver) can be synthesized in experiments [19–21]. To date, nanoshells have demonstrated their potential applications in *in vitro* and *in vivo* biological studies, ranging from light-triggered drug delivery and release [22] to whole-blood immunoassay diagnosis [23], to labeling the target molecules and photothermal therapy [24], and to molecular fluorescence enhancement [25,26]. Numerous experimental and theoretical studies have been reported on the one-photon fluorescence behaviors of molecules at the vicinity of nanoshells lying on the outside surface or encapsulated within the nanoshell [25–32]. However, the plasmonic-enhanced TPF with the metallic nanoshell is much underappreciated, and the systematically theoretical study of surface-enhanced TPF has seldom been reported.

In the present study, we investigate the single emitter-single nanoshell configurations systematically, and obtain comprehensive understandings of the TPF behaviors of single molecule both outside and inside a single nanoshell. Fluorophores labeled on the external surface and encapsulated inside the nanoshell present obviously different TPF emission behaviors. Simultaneous excitation and emission enhancements could be achieved by the suitable dimensions of the nanoshell. Several key parameters such as emitter's orientation and spectra overlaps between molecular band and plasmon resonances are also taken into account to optimize the enhancement effect. The result shows that the nanocomposite NS consisting fluorophores displays a promising candidate as a bright TPF probe that maybe versatile biolabels in fluorescence imaging applications.

2 Methods

We model the single emitter single nanoparticle system employing the finite-difference time-domain (FDTD) method [33,34]. The optical dielectric function of gold is modeled using the Drude Lorentz dispersion model [35] and the system is immersed in water. The refractive index is equal to 1.33 for water and 1.49 for silica without loss. An oscillating classical point dipole is considered as an isolated emitter. The presence of a metallic nanoshell modifies the radiative and nonradiative decay rates, thus altering the quantum efficiency of the nearby emitter. At the same time, the excitation optical intensity is also concentrated strongly near the gold nanoshell in comparison with the free space light. Then, the TPF signal of the isolated emitter is

$$S \propto k \cdot \sigma_{(\omega)}^{2p} \cdot \eta_{(\omega)} \cdot \left| p \cdot E \right|^4 ,$$

where k is the collection efficiency (assuming the signal is collected over all angles, and then it keeps the same with or without the nanoshell). For simplicity, the two-photon absorption cross-section σ^{2P} of the fluorophores is assumed to be wavelength independent, p is the transition electric dipole moment, and E is the electric field at the emitter position. $\eta_{(\omega)}$ is the quantum efficiency of the emitter which is related to η_0 (the quantum efficiency in free space) according to

$$\eta_{(\omega)} = \eta_{0(\omega)} \Big/ \left[\left(1 - \eta_{0(\omega)}\right) \Big/ F_{(\omega)} + \eta_{0(\omega)} \Big/ \eta_{a(\omega)} \right].$$

In the nanoscale system, the metal shell not only converts the optical energy into heat through the coupling of the surface plasmons, but also modifies the spontaneous emission rate of the emitter through the Purcell effect. Purcell factor (defined as normalized radiative decay rate) is simulated to characterize the enhancement of the radiative decay rate. Antenna efficiency, which is the power that reached the far field P_{rad} divided by the total emitting power of the dipole source P_{tot}, represents the quantum efficiency of the optical antenna; i.e., $\eta_{\mathrm{a}}=P_{\mathrm{rad}}/P_{\mathrm{tot}}\cdot P_{\mathrm{rad}}$ was obtained by integrating the Poynting vector over closed surfaces that contain the nanoantenna and dipolar source, while P_{tot} was obtained over closed surfaces containing the dipolar source only. The Purcell factor is related to emission and is defined as a nor-

malized ratio of radiative decay rates $F=P_{rad}/P_{rad,0}$. For the emission process, the excited state spontaneous decay process is determined by the antenna efficiency. For the excitation process, it should be much complicated to take full account of the excitation process from ground states to excited states, while the excitation EM field enhancement should be the main and direct effect. Then, the TPF brightness of the emitter studied is approximately only related to local field enhancement and the quantum efficiency.

3 Results and discussions

In plasmonic-enhanced fluorescence, the importance of spectral correlation between LSPRs modes of plasmonic nanostructures and fluorophores' absorption/emission bands has been convinced by numerous studies [25,32,36–38]. With increasing the particle size of nanoshells beyond the quasistatic limit, their dipolar plasmon resonances present systematic red-shift. At the same time, higher order multipolar resonances appear, because of the retardation effect by tuning the core/shell ratio and the dimension [39]. Here, NS-60-8 (nanoshell with a 60-nm core radius and an 8-nm thick shell) is studied in detail as its dipolar resonance lies at a wavelength of 880 nm and quadrupolar resonance at a wavelength of 700 nm. Because of the morphology of the core shell structure of nanoshell, the molecular TPF is differently enhanced inside or outside the metallic shell. This is related to the field distribution around the nanoshell, and the optical intensity distribution within the core region being much more uniform than that at the nanoshell outside. As for fluorescent probes being able to diffuse freely, the nanoshell constructs is an appealing candidate that can also accomplish the similar simultaneous excitation and emission enhancements of TPF.

The dipolar resonance lies in the near-infrared region (750–950 nm) according to the widely used TPF excitation source laser. The quadrupolar mode overlaps the emission maximum of Cy5.5 molecules (fluorophore widely used in biochemistry, emission maximum at wavelength of 700 nm and absorption maximum at wavelength of 670 nm as for one-photon process) [40]. The plasmon resonances of NS-60-8 are firstly calculated using plane wave illumination, and the nanoshell presents obvious dipolar and quadrupolar modes as shown in Figure 1. The quadrupolar resonance, which usually is the dark mode, can be excited directly with free-space incident light due to the retardation. For comparison, the plasmon resonance modes of the NS-60-8 are also calculated using a point source illumination outside and inside the NS. Two typical emitter-NS configurations are chosen for detailed investigation: (i) the dipole orientation along the radial axis placed at position A outside the nanoshell with the 10-nm dipole NS surface separation and (ii) the dipole placed at the center of the core region of the NS, which is indicated as the position B in Figure 1. When the point source is placed outside the nanoshell, the quadrupolar mode supported by NS-60-8 can be efficiently excited. It coincides with a previous paper that reported that the quadrupolar dark plasmon mode of a bipyramidal nanoparticle can induce a corresponding emission peak of a dipole source [41]. However, for the case of point source in the center of the core, it excites the plasmon resonance modes of the system symmetrically. Thus, only the dipolar resonance mode can be excited. In this situation, the quadrupolar mode is completely dark. The point source in different regions of the nanoshell can excite distinct plasmonic resonance modes. Thus, we can expect the TPF behavior to be influenced very differently for the fluorescent molecules located at various positions.

Figure 2 shows the calculated Purcell factor F, antenna efficiency η_a, quantum efficiency and relative TPF intensity for the emitter NS nanocomposite at positions A and B, respectively. Given that the initial quantum efficiency η_0 is 0.3 at λ=700 nm, we can calculate the relative fluorescence intensity of Cy5.5 excited by light at a wavelength of 880 nm in comparison with that in the absence of NS. The fluorescence properties display different features in the internal and external regions of the NS as shown in Figure 2. For the dipole source at position A, Purcell factor (Figure 2(a)) of the NS-60-8 displays a double-peak behavior at a wavelength of 880 nm and 700 nm separately, reflecting these two modes that are strongly radiating to the far field. Due to the presence of the quadrupolar plasmon resonance, the antenna efficiency has a hump around the wavelength 700 nm. While for the dipole at position B, the Purcell factor has only one characteristic peak as expected. However, the antenna efficiency keeps a high level in a very broad spectral range. For the dipole source at the core center of large NSs, the coupling strength of the dipole and the gold shell is relatively weak and the nonradiative loss due to the metal is small. Our calculations convince the previous results, i.e. a large core radius is desired to minimize the nonradiative damping and avoid significant quantum yield degradation of light emitters [31]. Therefore, position B provides a higher

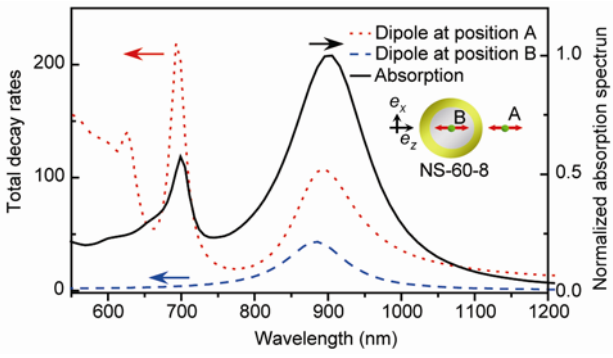

Figure 1 (Color online) Normalized total decay rates of a point dipole source near the nanoshell with a core radius of 60 nm and shell thickness of 8 nm. The dipole is placed outside the nanoshell with a 10-nm separation (dot). The dipole is in the center of the core (dash). Normalized absorption spectrum of NS-60-8 is also shown in the black curve.

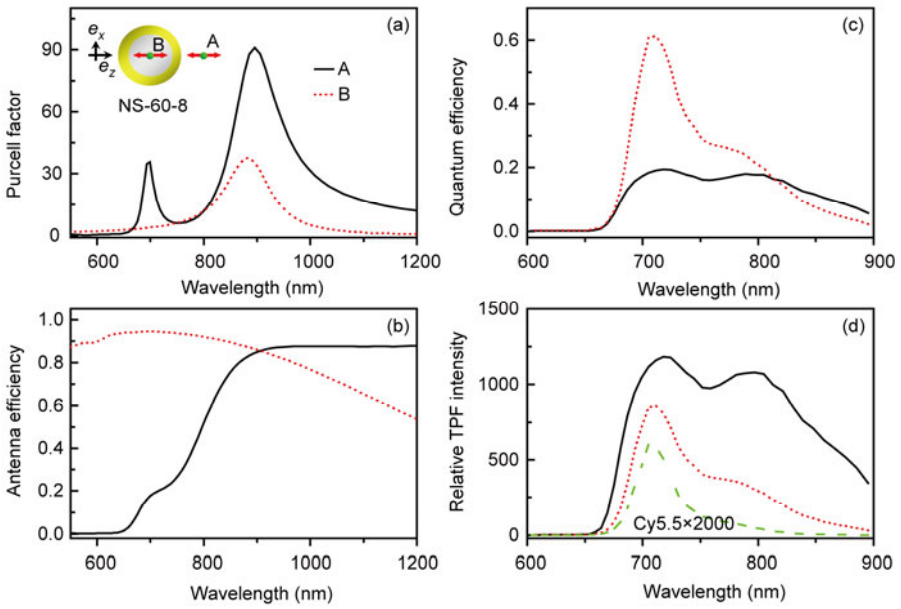

Figure 2 (Color online) Normalized Purcell factor F (a); antenna efficiency η_a (b); quantum efficiency of a single Cy5.5 dye (c) and the TPF intensity of Cy5.5 at two typical positions relative to the nanoshell (d). The relative fluorescence intensity of free Cy5.5 is plotted in dash for comparison.

quantum efficiency for Cy5.5 dye as shown in Figure 2(c). Unfortunately, high antenna efficiency usually means a faster radiative damping rate, which reduces the field enhancement, resulting in a weaker TPF intensity enhancement compared to Cy5.5 at the position A.

Next we investigate in detail how the relative position of the emitter outside or inside the NS influences the TPF behaviors. Figures 3(a) and (b) display the Purcell factor, the antenna efficiency separately at different distances between the emitter and the outer surface of the NS from 3 nm to 30 nm. The two-photon excitation enhancement (square of the local field enhancement), quantum efficiency of Cy5.5 and relative TPF intensity as a function of the emitter NS separation are demonstrated in Figures 3(c) and (d). The strength of the coupling increases greatly as the emitter NS separation decreases and the quantum yields decline rapidly due to the strong loss of metal at very small separations. Therefore, the optimal emitter NS distance is 5 nm for maximum TPF enhancement resulting from competition between the excitation and emission processes. Also, the TPF decrease if the fluorophore is very close to the metal surface with the separation less than 5 nm. The dipolar resonance of the NS can couple with the incident light resulting in a large localized field enhancement that increases the molecular excitation rate. At the same time, the radiative quadrupolar mode overlaps with the emission band of excited fluorophores (at a wavelength of 700 nm) to assist the fluorescence emission due to an enhancement in the quantum efficiency. Such dipole quadrupole jointly enhanced TPF has been demonstrated in our previous work, where the TPF of a single emitter is enhanced jointly by dipolar and quadrupolar modes of a single gold cylinder nanostructure on silica substrate [36]. The enhancement caused by excitation is particularly strong because of the quadratic dependence on the excitation intensity. Meanwhile, the emission enhancement at shorter wavelength plays an equally decisive role where the quadrupolar plasmonic mode helps the emission rate reducing the quenching effect of the metal.

Similar to the emitter outside, the TPF for the emitter located at various positions inside the NS is calculated in detail, and the results are summarized in Figure 4. Within the core region, the dipolar mode displays no changes at different positions (Figure 4(a)), which implies that the excitation rate enhancement is essentially the same and is accorded with the near-field distribution shown in the inset of Figure 5. The quadrupolar resonance gradually emerges as the emitter close to the internal surface of the gold NS. As the position of the point source is more off-center (i.e., being closer to the internal surface), the symmetry of the source NS geometry is broken so that the quadrupolar resonance mode couples with the source. The reduction of symmetry permits the original dark quadrupolar mode to be excited by the offset point source. However, the quadrupolar mode is a deteriorating mode for light emission process as there is an obvious dip at the corresponding position of the antenna efficiency (Figure 4(b)). Nevertheless, the antenna efficiency still keeps a high level in a broad spectral range. The distance dependence of the enhanced TPF emission is illustrated in Figures 4(c) and (d). According to the theoretical calculation, the optical field distribution within the core region is much more homogeneous compared to the external area of the nanoshell (which will be discussed later). The excitation rate enhancement for various positions presents slight differences, whereas the quantum efficiency gradually

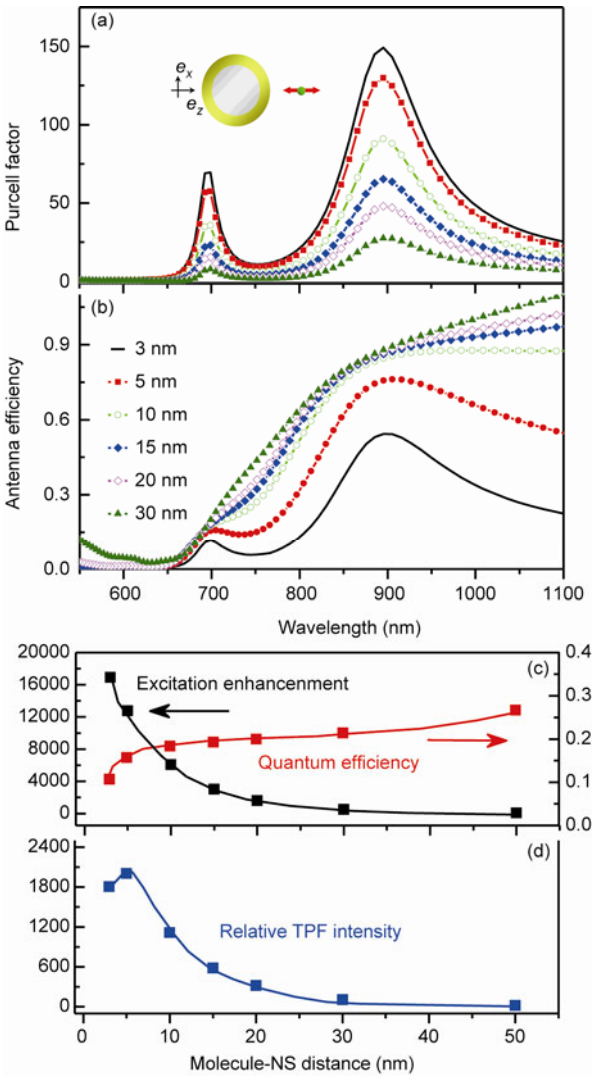

Figure 3 (Color online) Position evolution of Purcell Factor (a) and antenna efficiency (b) for an emitter outside coupled to the nanoshell "NS-60-8". The separation between the emitter and the external shell of the nanoshell is set to 3 nm, 5 nm, 10 nm, 15 nm, 20 nm, and 30 nm, respectively. The two-photon excitation enhancement (square of the local field enhancement), quantum efficiency of Cy5.5, and relative TPF intensity as a function of the emitter NS separation are demonstrated in (c) and (d).

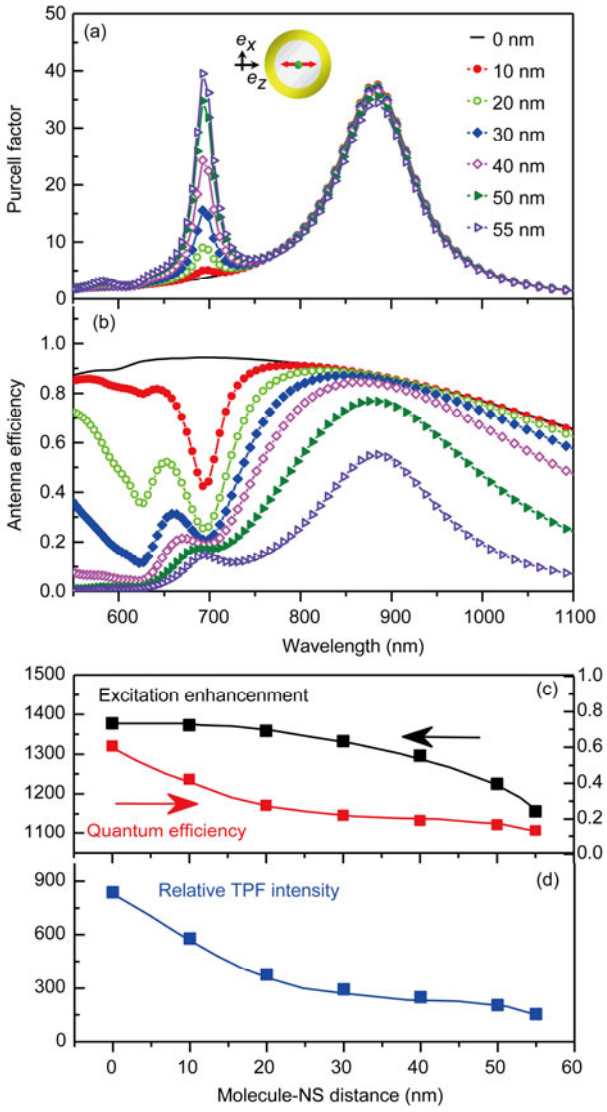

Figure 4 (Color online) Position evolution of the Purcell Factor (a) and antenna efficiency (b) for an emitter inside coupled to the nanoshell. The distance of the emitter with the center of the core is set to 0 nm, 10 nm, 20 nm, 30 nm, 40 nm, 50 nm, and 55 nm. The two-photon excitation enhancement, quantum efficiency of Cy5.5, and relative TPF intensity as a function of the emitter NS distance are demonstrated in (c) and (d).

declines due to the metal loss when the emitter is being close to the gold shell. Hence, the TPF signal presents a similar declining trend. Thus, for a bright probe, the encapsulated fluorescence dye should be imbedded around the center of the dielectric core of the NS, and separated from the internal metallic surface.

Generally, fluorescent molecules outside the NS can possess much greater excitation enhancement, but it is very sensitive to the distance from the NS surface. Meanwhile, the quantum efficiency is much lower than the emitters encapsulated inside the NS. Taking into account that the TPF intensity depends not only on the local field but also on the quantum efficiency, bonding the fluorescent molecules outside the NS surface to obtain the high fluorescence signal needs to precisely control the molecule separations and orientations. However, significantly TPF remains possible if we encapsulate molecules inside the NS. The TPF intensity of single molecule in the center of the NS has the comparable value with the molecule conjugated outside with 10 nm separation. In fact, embedding dye molecules inside may even be better because the particle can encapsulate large number of molecules, and the molecules can provide satisfied TPF signal intensity without the limit of molecule orientation.

The advantages of encapsulating fluorescent molecules inside the NS can be further demonstrated by the studies on how the dipole orientations influence on the fluorescence intensity. This can also help us to have a deeper and full

understanding of the plasmonic-enhanced TPF of the emitter NS system. All the previous calculations were performed for an emitter orientated along the z direction and moved on the radial axis in cylindrical coordinates. Now 3D-FDTD calculations have to be performed to investigate the effects of different orientations of a single emitter relative to the NS construct. A dipole is then placed at various positions with different orientations to the NS-60-8. Because of the NS's rotational symmetry, only two orientations denoted as e_z and e_x needed to be considered (precisely e_z refers to the radial axis, whereas e_x refers to the axis perpendicular to the radial one). The typical results show that the orientation dependence of the fluorescence within the NS core region present distinct behaviors compared with that outside the NS.

Figure 5 shows the position evolution of F, η_a, and the TPF intensity, and the trends are consistent with those results obtained using 2D calculations, except for the differences of absolute values. The optical field distribution of the NS-60-8 illuminated by planar continuous waves polarized along the z direction at a wavelength of 880 nm is calculated and plotted in the inset of Figure 5 for a better understanding of the orientation and configuration dependent phenomena. The left of Figure 5 concerns the emitters that are placed outside. There is a strong molecular orientation dependence of the plasmonic-enhanced TPF. The emitter oriented along the e_z has much stronger coupling efficiency with the NS and presents a significantly larger enhancement than that placed at the same position while oriented along the e_x direction. However, for the emitters placed within the NS core region shown in the right panel, the molecules with polarization along the e_z present similar Purcell factor and antenna efficiency as the ones polarized along e_x. Then, the fluorescent emitters embedded within the NS can experi-

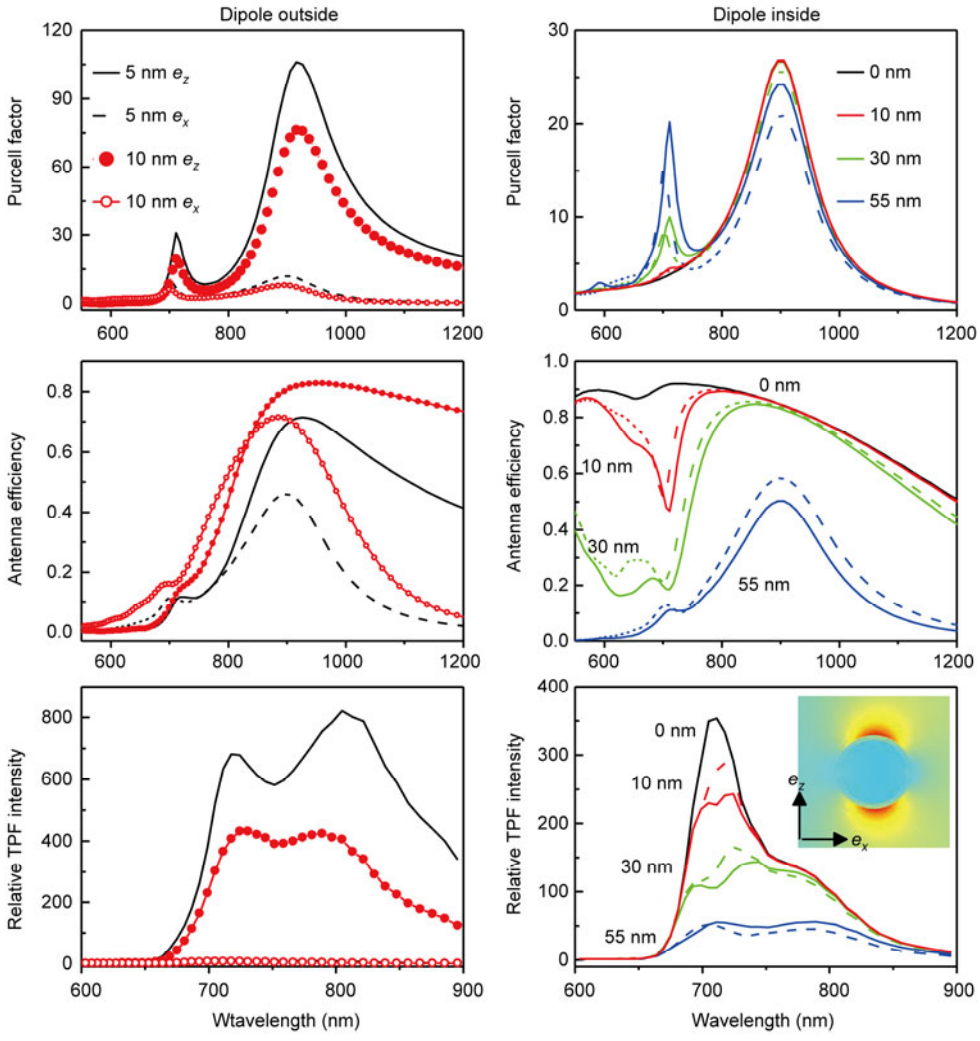

Figure 5 (Color online) Purcell factor, antenna efficiency and two-photon intensity. The emitter is placed outside (left panel) or inside (right panel) the "NS-60-8". The solid and dashed curves represent the orientation of the dipole with e_z and e_x orientation. The separation between the emitter and the nanoshell outer surface is fixed at 5 nm and 10 nm when the emitter is placed outside. The separation between the emitter and the center of the nanoshell is fixed at 0 nm, 10 nm, 30 nm, and 55 nm when the emitter is placed inside the NS. The inset shows the field distributions in the x-z plane near the NS-60-8. The excitation light polarizes along the z direction with an excitation wavelength of 880 nm.

ence the same substantial fluorescence enhancement regardless of the molecular orientations. This is consistent with the characteristics of the optical field distribution within the NS, i.e. it presents slight differences under different polarized illumination, for instance, polarized along the e_x or e_z directions (data not shown here). In addition, it should be noted that the plasmonic nanostructures can absorb the illuminated incident light that could lead to a plasmon emission directly as two-photon luminescence. Also, there is often a strong localized electric field on the surface of the plasmonic nanostructures which could enable some nonlinear optical effects, like second harmonic generation or four-wave mixing processes [42,43]. However, our theoretical simulations do not include such probable factors that could affect the two-photo fluorescence process significantly during the interaction between metallic nanostructures and nearby fluorophores.

4 Conclusions

Summary, we theoretically present a promising bright probe using gold nanoshell to improve the TPF performances. Fluorescent emitters placed outside the nanoshell can reach higher fluorescence intensities near the surface when their orientations coincide with that of the light polarization, but the TPF enhancement decays rapidly with the increase of distance between the emitter and the shell surface. While fluorescent emitters embedded inside the NS can experience substantial TPF enhancement without strict requirements of the position and dipole orientations, the radiative light can be coupled efficiently with the far field. Besides, the metal shell protects the encapsulated fluorophores from the external environment. The stability of fluorophores can be improved by the strong coupling between the fluorophores and the NS resulting in a shorter fluorescence lifetime. These considerations suggest that fluorophores encapsulated in metallic nanoshells is a more desirable nanocomposite configuration for the TPF probe in bioimaging applications.

This work was supported by the National Key Basic Research Program of China (Grant No. 2013CB328703) and the National Natural Science Foundation of China (Grant Nos. 11374026, 91221304 and 11121091).

1 Helmchen F, Denk W. Deep tissue two-photon microscopy. Nat Methods, 2005, 2(12): 932–940
2 So P T C, Dong C Y, Masters B R, et al. Two-photon excitation fluorescence microscopy. Annu Rev Biomed Eng, 2000, 2: 399–429
3 Yao S, Belfield K D. Two-photon fluorescent probes for bioimaging. Eur J Org Chem, 2012, 2012(17): 3199–3217
4 Santra S, Malhotra A. Fluorescent nanoparticle probes for imaging of cancer. Wiley Interdiscip Rev Nanomed Nanobiotechnol, 2011, 3(5): 501–510
5 Larson D R, Zipfel W R, Williams R M, et al. Water-soluble quantum dots for multiphoton fluorescence imaging *in vivo*. Science, 2003, 300: 1434–1436
6 Yong K T, Qian J, Roy I, et al. Quantum rod bioconjugates as targeted probes for confocal and two-photon fluorescence imaging of cancer cells. Nano Lett, 2007, 7(3): 761–765
7 Jung J M, Yoo H W, Stellacci F, et al. Two-photon excited fluorescence enhancement for ultrasensitive DNA detection on large-area gold nanopatterns. Adv Mater, 2010, 22(23): 2542–2546
8 Fischer J, Bocchio N, Unger A, et al. Near-field-mediated enhancement of two-photon-induced fluorescence on plasmonic nanostructures. J Phys Chem C, 2010, 114(49): 20968–20973
9 Hartling T, Reichenbach P, Eng L M. Near-field coupling of a single fluorescent molecule and a spherical gold nanoparticle. Opt Express, 2007, 15(20): 12806–12817
10 Lakowicz J R. Plasmonics in biology and plasmon-controlled fluorescence. Plasmonics, 2006, 1(1): 5–33
11 Fu Y, Zhang J, Lakowicz J R. Plasmon-enhanced fluorescence from single fluorophores end-linked to gold nanorods. J Am Chem Soc, 2010, 132(16): 5540–5541
12 Swierczewska M, Lee S, Chen X Y. The design and application of fluorophore-gold nanoparticle activatable probes. Phys Chem Chem Phys, 2011, 13(21): 9929–9941
13 Moroz A. Spectroscopic properties of a two-level atom interacting with a complex spherical nanoshell. Chem Phys, 2005, 317(1): 1–15
14 Guzatov D V, Klimov V V. Radiative decay engineering by triaxial nanoellipsoids. Chem Phys Lett, 2005, 412(4-6): 341–346
15 Girard C, Martin O J F, Leveque G, et al. Generalized bloch equations for optical interactions in confined geometries. Chem Phys Lett, 2005, 404(1-3): 44–48
16 Wenger J, Gerard D, Dintinger J, et al. Emission and excitation contributions to enhanced single molecule fluorescence by gold nanometric apertures. Opt Express, 2008, 16(5): 3008–3020
17 Tian X, Tong L, Xu H. New progress of plasmonics in complex metal nanostructures. Sci China-Phys Mech Astron, 2013, 56(12): 2327–2336
18 Zheng H, Xu L, Zhang Z, et al. Fluorescence enhancement of acridine orange in a water solution by Au nanoparticles. Sci China-Phys Mech Astron, 2010, 53(10): 1799–1804
19 Oldenburg S J, Averitt R D, Westcott S L, et al. Nanoengineering of optical resonances. Chem Phys Lett, 1998, 288(2-4): 243–247
20 Lal S, Link S, Halas N J. Nano-optics from sensing to waveguiding. Nat Photonics, 2007, 1(11): 641–648
21 Zhou X, Fang J, Liao X, et al. Influence of structural defects on the optical properties of strongly coupled Au nanoshell arrays. Sci China-Phys Mech Astron, 2013, 56(9): 1664–1669
22 West J L, Halas N J. Engineered nanomaterials for biophotonics applications: Improving sensing, imaging, and therapeutics. Annu Rev Biomed Eng, 2003, 5: 285–292
23 Hirsch L R, Jackson J B, Lee A, et al. A whole blood immunoassay using gold nanoshells. Anal Chem, 2003, 75(10): 2377–2381
24 Loo C, Lowery A, Halas N J, et al. Immunotargeted nanoshells for integrated cancer imaging and therapy. Nano Lett, 2005, 5(4): 709–711
25 Tam F, Goodrich G P, Johnson B R, et al. Plasmonic enhancement of molecular fluorescence. Nano Lett, 2007, 7(2): 496–501
26 Jin Y D, Gao X H. Plasmonic fluorescent quantum dots. Nat Nanotechnol, 2009, 4(9): 571–576
27 Zaiba S, Lerouge F, Gabudean A M, et al. Transparent plasmonic nanocontainers protect organic fluorophores against photobleaching. Nano Lett, 2011, 11(5): 2043–2047
28 Zhang J, Gryczynski I, Gryczynski Z, et al. Dye-labeled silver nanoshell-bright particle. J Phys Chem B, 2006, 110(18): 8986–8991
29 Bardhan R, Grady N K, Halas N J. Nanoscale control of near-infrared fluorescence enhancement using Au nanoshells. Small, 2008, 4(10): 1716–1722
30 Enderlein J. Theoretical study of single molecule fluorescence in a metallic nanocavity. Appl Phys Lett, 2002, 80(2): 315–317
31 Miao X Y, Brener I, Luk T S. Nanocomposite plasmonic fluorescence emitters with core/shell configurations. J Opt Soc Am B, 2010, 27(8): 1561–1570
32 Zhang T, Lu G, Li W, et al. Optimally designed nanoshell and matryoshka-nanoshell as a plasmonic-enhanced fluorescence probe. J

Phys Chem C, 2012, 116(15): 8804–8812
33 Taflove A, Hagness S C. Computational Electrodynamics: The Finite-Difference Time-Domain Method. 3rd ed. Boston: Artech House, 2005
34 Mohammadi A, Kaminski F, Sandoghdar V, et al. Fluorescence enhancement with the optical (bi-) conical antenna. J Phys Chem C, 2010, 114(16): 7372–7377
35 Johnson P B, Christy R W. Optical constants of noble metals. Phys Rev B, 1972, 6(12): 4370–4379
36 Zhang T, Lu G, Liu J, et al. Strong two-photon fluorescence enhanced jointly by dipolar and quadrupolar modes of a single plasmonic nanostructure. Appl Phys Lett, 2012, 101(5): 051109
37 Munechika K, Chen Y, Tillack A F, et al. Spectral control of plasmonic emission enhancement from quantum dots near single silver nanoprisms. Nano Lett, 2010, 10(7): 2598–2603
38 Pompa P P, Martiradonna L, Della Torre A, et al. Metal-enhanced fluorescence of colloidal nanocrystals with nanoscale control. Nat Nanotech, 2006, 1(2): 126–130
39 Oldenburg S J, Jackson J B, Westcott S L, et al. Infrared extinction properties of gold nanoshells. Appl Phys Lett, 1999, 75(19): 2897–2899
40 Buschmann V, Weston K D, Sauer M. Spectroscopic study and evaluation of red-absorbing fluorescent dyes. Bioconjugate Chem, 2003, 14(1): 195–204
41 Liu M, Lee T W, Gray S, et al. Excitation of dark plasmons in metal nanoparticles by a localized emitter. Phys Rev Lett, 2009, 102(10): 107401
42 Zhang Y, Grady N K, Ayala-Orozco C, et al. Three-dimensional nanostructures as highly efficient generators of second harmonic light. Nano Lett, 2011, 11(12): 5519–5523
43 Palomba S, Novotny L. Near-field imaging with a localized nonlinear light source. Nano Lett, 2009, 9(11): 3801–3804